

# Optical management in high-efficiency thin-film silicon micromorph solar cells with a silicon oxide based intermediate reflector

Didier Dominé<sup>\*</sup>, Peter Buehlmann, Julien Bailat, Adrian Billet, Andrea Feltrin, and Christophe Ballif

Institute of Microtechnology (IMT), University of Neuchâtel, Rue A.-L. Breguet 2, 2000 Neuchâtel, Switzerland

Received 4 June 2008, revised 24 June 2008, accepted 24 June 2008

Published online 7 July 2008

PACS 68.35.Ct, 78.66.–w, 78.66.Jg, 84.60.Bk, 84.60.Jt

\* Corresponding author: e-mail [didier.domine@unine.ch](mailto:didier.domine@unine.ch), Phone: +41 32 718 33 12, Fax: +41 32 718 32 01

In the effort to increase the stable efficiency of thin film silicon micromorph solar cells, a silicon oxide based intermediate reflector (SOIR) layer is deposited *in situ* between the component cells of the tandem device. The effectiveness of the SOIR layer in increasing the photo-carrier generation in the a-Si:H top absorber is compared for p–i–n devices deposited on different rough, highly transparent, front ZnO layers. High haze and low doping level for the front ZnO

strongly enhance the current density ( $J_{sc}$ ) in the  $\mu\text{c-Si:H}$  bottom cell whereas  $J_{sc}$  in the top cell is influenced by the angular distribution of the transmitted light and by the reflectivity of the SOIR related to different surface roughness. A total  $J_{sc}$  of  $26.8 \text{ mA/cm}^2$  and an initial conversion efficiency of 12.6% are achieved for  $1.2 \text{ cm}^2$  cells with top and bottom cell thicknesses of 300 nm and 3  $\mu\text{m}$ , and without any anti-reflective coating on the glass.

© 2008 WILEY-VCH Verlag GmbH & Co. KGaA, Weinheim

The micromorph solar cell concept consists of an optical and electrical series connection of a high-gap a-Si:H top cell and a low-gap  $\mu\text{c-Si:H}$  bottom cell. To minimize light-induced degradation, the thickness of the a-Si:H absorber should not exceed 300 nm. This constraint considerably limits the short-circuit current density ( $J_{sc}$ ) on the top cell and, hence, the efficiency of the whole device. Therefore an intermediate reflecting layer (IRL) between the individual cells must be introduced to increase the current in the a-Si:H absorber [1–4].

In this letter, we first analyze the light scattering properties of nano-textured transparent conductive oxide (TCO) layers used as front electrodes for micromorph cells deposited in the superstrate configuration (p–i–n). Photocurrents in individual state-of-the-art cells with a Si oxide based IRL (SOIR) are then compared for front TCOs with different surface morphologies and the observed differences are related to the optical characteristics of these TCOs.

The three types of TCO (type-A, -B and -C) used in this study are as-grown surface textured ZnO films with two different doping levels obtained by low-pressure chemical vapour deposition (LPCVD) on Schott AF45

glass substrates. The thickness of the resulting layers is adjusted to obtain a sheet resistance below  $10 \Omega/\text{sq}$ . The root mean square value of their surface roughness ( $\sigma_{rms}$ ) and the correlation length  $\xi$  of the textured surface are determined by atomic force microscopy. These characteristics, summarized in Table 1, depend on the thickness of the layers and on the duration of a plasma post-treatment [5] applied to their surface. Note that the type-B ZnO (without post-treatment), whose sharp V-shape structures prevent good electrical properties of the device [5], is presented only for the sake of light scattering comparisons. The low doping level used for deposition of the thick large-grain ZnO layers (type-B and -C) provides high transparency in the near infrared (NIR) spectral range because of reduced free carrier absorption (FCA) [6]. The diffuse transmittance in-air of the different TCOs, when light is normally incident to the glass side, is investigated by two methods. First, the haze factor for transmitted light  $H_T = T_{dif}/T_{tot}$  is calculated from total and diffuse optical transmittance ( $T_{tot}$  and  $T_{dif}$ ) measurements carried out with a photo-spectrometer equipped with an integration-sphere. Second, the intensity per unit of solid angle scattered at an angle  $\theta$  with respect to the direction of an incident laser beam (633 nm) is de-

**Table 1** Thickness  $d$ , carrier concentration  $N$  [6], surface roughness  $\sigma_{\text{rms}}$ , correlation length  $\xi$ , and characteristic morphology of the valleys for the type-A, -B and -C front ZnO layers.

| front ZnO type             | A                    | B                  | C                  |
|----------------------------|----------------------|--------------------|--------------------|
| $d$ ( $\mu\text{m}$ )      | 1.9                  | 4.8                | 4.8                |
| $N$ ( $\text{cm}^{-3}$ )   | $1.4 \times 10^{20}$ | $4 \times 10^{19}$ | $4 \times 10^{19}$ |
| $\sigma_{\text{rms}}$ (nm) | 66                   | 178                | 165                |
| $\xi$ ( $\mu\text{m}$ )    | 0.4                  | 0.8                | 0.8                |
| morphology of valleys      | V-shape              | V-shape            | U-shape            |

terminated by angular resolved scattering (ARS) measurement with a rotating photo-detector.

P-i-n micromorph cells and SOIR [3] layers are deposited by very-high frequency plasma enhanced chemical vapour deposition (VHF-PECVD). For the tandem cells presented in the first part of this letter, the top a-Si:H cells are deposited in a KAI-S reactor from OC Oerlikon. The SOIR layers and the bottom  $\mu\text{c-Si:H}$  cells are then deposited in a laboratory-scale dual chamber VHF-PECVD system. The state-of-the-art micromorph cells presented at the end are fully completed in this dual chamber system. The back contact of the cells consists of a LPCVD ZnO layer covered with a white dielectric reflector [7]. The cell area ( $\sim 1.2 \text{ cm}^2$ ) is patterned by  $\text{SF}_6$  plasma etching.

External quantum efficiencies (EQE) of the top and bottom cells ( $\text{EQE}_{\text{top}}$  and  $\text{EQE}_{\text{bot}}$ ) are measured under red and blue bias-light illumination, respectively. The corresponding  $J_{\text{sc}}$  values ( $J_{\text{sc, top}}$  and  $J_{\text{sc, bot}}$ ) are calculated from the EQE curves and the AM1.5 g solar spectrum. Current density–voltage ( $J$ – $V$ ) curves are measured using a dual lamp sun simulator (Wacom) in standard test conditions ( $25^\circ\text{C}$ , AM1.5 g spectrum,  $100 \text{ mW/cm}^2$ ).  $J$  is normalised with the  $J_{\text{sc}}$  value deduced from the EQE measurements.

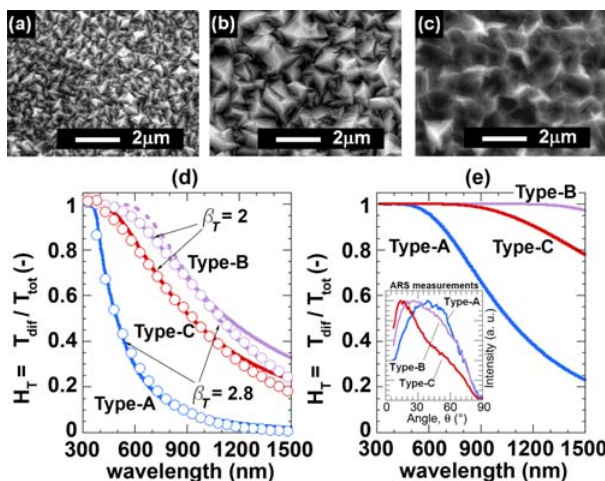


**Figure 1** (online colour at: [www.pss-rapid.com](http://www.pss-rapid.com)) (a)–(c) SEM pictures of typical type-A, -B and -C ZnO layers. Experimental (symbols) and calculated (lines) haze in transmission (d) in air and (e) at the ZnO/Si interface for the type-A, -B and -C front ZnO layers. The inset in (e) shows ARS measurements in-air.

For the TCOs presented in Table 1, the experimental haze factors  $H_T$  are plotted in Fig. 1(d) as a function of the wavelength  $\lambda$  of the transmitted light. The experimental data can be fitted by a function relating  $H_T$  to the surface roughness  $\sigma_{\text{rms}}$  [8, 9]:

$$H_T(\lambda) = 1 - \exp[-(4\pi\sigma_{\text{rms}}C_T|n_1 - n_2/\lambda)^{\beta_T}] \quad (1)$$

where  $n_1$  and  $n_2$  are the refractive indices of the incident and transmission media, respectively, and  $C_T$ ,  $\beta_T$  are fitting parameters. For the LPCVD ZnO layers used in this study, the fits obtained with  $C_T$  between 0.42 and 0.53 are plotted in Fig. 1(a). Defining  $\lambda_{\text{eff}}$  as  $\lambda/|n_1 - n_2|$ , an almost cubic dependence ( $\beta_T = 2.8$ ) on the factor  $\sigma_{\text{rms}}/\lambda_{\text{eff}}$  in the exponential is found for the type-A ZnO (small feature size). This is in agreement with Zeman et al. who found a cubic dependence on  $\sigma_{\text{rms}}/\lambda_{\text{eff}}$  for  $H_T$  of Asahi U-type  $\text{SnO}_2:\text{F}$  layers (similar to type-A ZnO) [9], whereas a square dependence and  $C_T = 0.5$  are predicted by the scalar scattering theory [10]. For type-B and type-C ZnO layers (large feature size),  $H_T$  is described by a square dependence on  $\sigma_{\text{rms}}/\lambda_{\text{eff}}$  for  $\lambda < 900 \text{ nm}$ , as predicted by theory. But for larger  $\lambda$ , an almost cubic dependence is found again. Note that Stiebig et al. mentioned power factors larger than 3 for ZnO:Al layers textured by post-etching in HCl [8].

The spectral dependence of  $H_T$  at the internal ZnO/Si interface, as calculated from Eq. (1) using  $n_2 = 4$  for Si and values deduced from the measurements in air for  $C_T$  and  $\beta_T$ , are plotted in Fig. 1(e). This indicates that, in a device, more than 65%, 95% and 100% of the light with  $\lambda < 900 \text{ nm}$  would be diffused by ZnO of type-A, -C and -B.

Angular distributions (normalized to their maximum values) of the diffuse light ( $\lambda = 633 \text{ nm}$ ) transmitted in air through the TCOs indicate scattering at wider angles for the type-A ZnO (inset in Fig. 1(e)). Assuming that ARS in air is relevant to predict the ZnO/Si internal interface behaviour [11], this more favourable angular distribution offsets the slightly lower  $H_T$  value at a ZnO/Si interface for  $\lambda < 900 \text{ nm}$ . This explains why the less diffusive type-A ZnO is more suited for light trapping in a-Si:H single junction solar cells than the type-C ZnO, as observed in a previous work for the 550–700 nm spectral range [2].

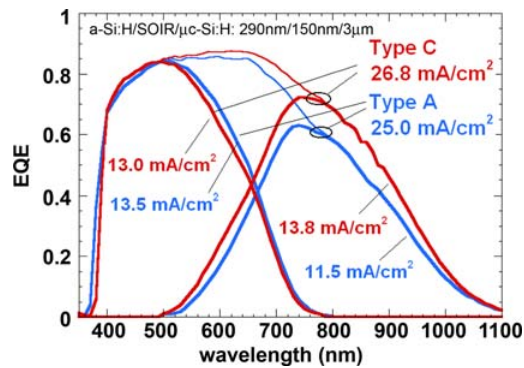


**Figure 2** (online colour at: [www.pss-rapid.com](http://www.pss-rapid.com)) EQEs of micromorph cells with 150 nm thick SOIR layers deposited on type-A and type-C front ZnO layers.

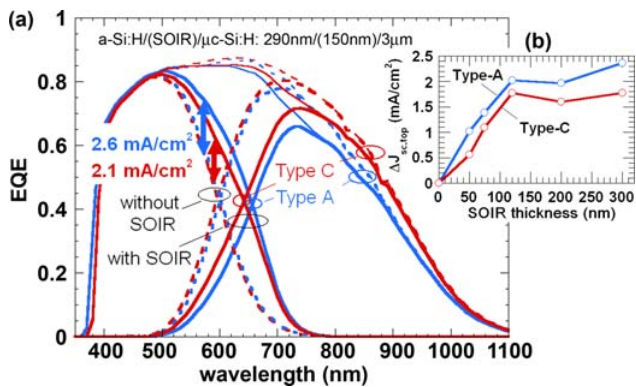


**Figure 3** (online colour at: www.pss-rapid.com) (a) EQEs of micromorph cells with and without a 150 nm thick SOIR deposited on type-A and type-C front ZnO layers. (b) Gains obtained in  $J_{sc,top}$  for a thickness series of SOIR layers.

EQEs of micromorph tandems deposited on type-A and type-C ZnO layers, with top cell, SOIR, and bottom cell thicknesses of 290 nm, 150 nm, and 3  $\mu\text{m}$ , respectively, are plotted in Fig. 2. The sum of the  $J_{sc}$  values of the individual cells is increased by 7% from 25.0  $\text{mA}/\text{cm}^2$  to 26.8  $\text{mA}/\text{cm}^2$  when the tandem is deposited on the thick ZnO. The gain in EQE occurs in the red and NIR parts of the spectrum as a result of the increased  $H_T$  (shown in Fig. 1) and low FCA of the thick and lightly doped type-C ZnO. However,  $J_{sc,top}$  is smaller for the device deposited on this thicker ZnO layer. This is examined in the following.

EQEs of four micromorph cells, with and without SOIR, deposited on type-A and type-C ZnO, are plotted in Fig. 3(a). Comparable  $\text{EQE}_{top}$  curves are obtained when no IRL is present. But the gain in  $J_{sc,top}$  ( $\Delta J_{sc,top}$ ) obtained by insertion of the IRL is larger (2.6 instead of 2.1  $\text{mA}/\text{cm}^2$ ) when the tandem is deposited on the type-A (smaller feature size) compared to the type-C ZnO.  $\Delta J_{sc,top}$  versus the thickness of the SOIR layer inserted in devices with top and bottom cell thicknesses of 180 nm and 1.8  $\mu\text{m}$ , respectively, is plotted in Fig. 3(b). With the type-A ZnO,  $\Delta J_{sc,top}$  is indeed systematically  $\sim 0.5 \text{ mA}/\text{cm}^2$  larger than with type-C. The  $\text{EQE}_{top}$  curves for the two devices without IRL in Fig. 3(a) are almost identical because of the absence of optical interface between the top and bottom cell. Indeed, in this case, light with  $\lambda \sim 600 \text{ nm}$  travels only once through the Si layers, making ineffective any better light scattering capability of the front TCO at this wavelength.

These observations indicate that the larger  $J_{sc,top}$  values reported in Fig. 2 and in a previous work [2] when the micromorph with IRL is deposited onto a ZnO layer with small feature size is caused by a better effectiveness of the IRL. On one hand this is due to a sufficient  $H_T$  ( $>80\%$ ) at the TCO/Si interface in the 550–700 nm spectral range combined with an improved ARS distribution, as shown in Fig. 1(e) for the type-A ZnO. This combination enhances the light trapping promoted by the IRL in the top cell. On the other hand, difference in steepness of the index change

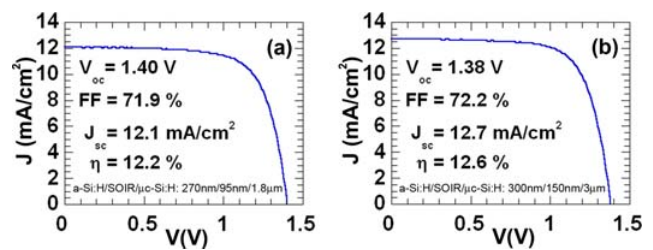


**Figure 4** (online colour at: www.pss-rapid.com)  $J$ – $V$  curves of 1.2  $\text{cm}^2$  state-of-the-art micromorph cells with a bottom cell thickness of (a) 1.8  $\mu\text{m}$  and (b) 3.0  $\mu\text{m}$ .

at the rough Si/IRL interface, considered as non abrupt in an effective medium approximation [2], also influences the effectiveness of the IRL. This effect seems less important in view of the similar slopes in  $\Delta J_{sc,top}$  for the two types of ZnO, in Fig. 3(b), with IRLs thicker than 50 nm.

Note that losses by increased total reflectance of the cell are observed when an IRL is inserted [3], as indicated by the sum of  $\text{EQE}_{top}$  and  $\text{EQE}_{bot}$  curves in Fig. 3(a).

For state-of-the-art micromorph cells deposited on type-C ZnO layers, with a bottom cell thickness of 1.8  $\mu\text{m}$  and 3.0  $\mu\text{m}$ , initial conversion efficiencies of 12.2% and 12.6% are achieved, respectively. The  $J$ – $V$  characteristics of these micromorph cells are represented in Fig. 4. The thinner device is top limited and provides an open-circuit voltage  $V_{oc}$  of 1.4 V. With the thicker  $\mu\text{c-Si:H}$  absorber a bottom limited micromorph cell ( $J_{sc,top} = 13.3 \text{ mA}/\text{cm}^2$ ) with  $J_{sc} = 12.7 \text{ mA}/\text{cm}^2$  is obtained.

In summary, a gain in  $J_{sc,top}$  of 2.6  $\text{mA}/\text{cm}^2$  is obtained with a SOIR layer deposited *in situ*. This is comparable to previous results with an *ex situ* ZnO layer [2]. This gain depends on the surface morphology of the front TCO and therefore higher  $J_{sc,top}$  values are achieved with the LPCVD ZnO layer with small feature size. However, when the rougher TCO is used, a remarkably high 26.8  $\text{mA}/\text{cm}^2$  value is obtained for the sum of  $J_{sc}$ , because of the combined benefits of low FCA and large haze in the NIR. Our best bottom limited micromorph cell (1.2  $\text{cm}^2$ ) with 12.6% initial conversion efficiency is deposited on this TCO, without any antireflection coating on the glass.

**Acknowledgement** This work was supported by the Swiss Federal Energy Office (OFEN) (contracts 101191 and 153032) and by the EU (Athlet Project, contract 019670).

## References

- [1] D. Fisher et al., Proc. of the 25<sup>th</sup> IEEE PVSC, 1996, p. 1053.
- [2] D. Dominé et al., Proc. of the 4<sup>th</sup> WCPEC, 2006, p. 1465.
- [3] P. Buehlmann et al., Appl. Phys. Lett. **91**, 143505 (2007).
- [4] K. Yamamoto et al., Prog. Photovoltaics **13**, 645 (2005).
- [5] J. Bailat et al., Proc. of the 4<sup>th</sup> WCPEC, 2006, p. 1533.
- [6] J. Steinhauser et al., Appl. Phys. Lett. **90**, 142107 (2007).
- [7] J. Meier et al., Proc. of the 31<sup>st</sup> IEEE PVSC, 2005, p. 1464.
- [8] H. Stiebig et al., Proc. of the 16<sup>th</sup> EU PVSEC, 2000, p. 549.
- [9] M. Zeman et al., J. Appl. Phys. **88**, 6436 (2000).
- [10] C. K. Carniglia, Opt. Eng. **18**, 104 (1979).
- [11] J. Krc et al., J. Appl. Phys. **92**, 749 (2002).